An electro-osmotic microfluidic system to characterize cancer cell migration under confinement

T.H. Hui[1], W.C. Cho[2], H.W. Fong[2], M. Yu[3], K.W. Kwan[1], K.C. Ngan[2], K.H. Wong[2], Y. Tan[4], S. Yao[3], H. Jiang[5*], Z. Gu[6,7*] and Y. Lin[1*]

[1] Department of Mechanical Engineering, The University of Hong Kong, Hong Kong SAR, China

[2] Department of Clinical Oncology, Queen Elizabeth Hospital, Hong Kong SAR, China

[3] Department of Mechanical and Aerospace Engineering, Hong Kong University of Science and Technology, Hong Kong SAR, China

[4] Interdisciplinary Division of Biomedical Engineering, The Hong Kong Polytechnic University, Hong Kong SAR, China.

[5] Department of Modern Mechanics, University of Science and Technology of China, Hefei, China

[6] Shum Yiu Foon Shum Bik Chuen Memorial Centre for Cancer and Inflammation Research, School of Chinese Medicine, Hong Kong Baptist University, Hong Kong SAR, China.

[7] Department of Cancer Biology, Dana-Farber Cancer Institute, Boston, MA

* Corresponding authors: ylin@hku.hk, zhizhan_gu@hkbu.edu.hk, jianghy@ustc.edu.cn

Abstract

We have developed a novel electro-osmotic microfluidic system to apply precisely controlled osmolarity gradients to cancer cells in micro-channels. We observed that albeit adhesion is not required for cells to migrate in such a confined microenvironment, the migrating velocity of cells is strongly influenced by the interactions between the cells and the channel wall, with a stronger adhesion leading to diminished cell motility. Furthermore, through examining more than 20 different types of cancer cells, we found a linear positive correlation between the protein concentration of the aquaporin-4 (AQP4) and the cell migrating speed. Knockdown of AQP4 in invasive re-populated cancer stem cells reduced their migration capability down to the level that is comparable to their parental cancer cells. Interestingly, these observations can all be quantitatively explained by the osmotic engine model where the cell movement is assumed to be driven by cross-membrane ion/water transport while adhesion acts as a frictional resistance against the cell motility. By providing versatile and controllable features in regulating and characterizing the migration capability of cells, our system may serve as a useful tool in quantifying how cell motility is influenced by different physical and biochemical factors, as well as elucidating the mechanisms behind, in the future.

1. Introduction

During metastasis, cancer cells need to significantly alter their shapes and internal cellular structures in order to travel through physical barriers like dense matrices, vasculatures and capillaries [1-3]. Various *in vitro* methods such as wound healing, microliter-scale migration and trans-well invasion assays have been developed to quantify tumors cell invasion [4]. Unfortunately, most of these cell migration or invasion assays only quantify cell motilities on open 2D surfaces without physical confinement, which do not perfectly mimic those dense tissue microenvironments *in vivo*. Hence, recently, microfluidic devices have become increasingly popular in characterizing cell motilities in narrow confined microchannels [5, 6]. In particular, with the rapid development of micro-fabrication/device technologies, more and more examples of such approach in clinical applications have been reported/suggested [7-10].

Previous findings suggested that cells utilize their actomyosin contraction and protrusion, cooperating with the cell adhesions to extracellular matrices, to crawl over surfaces [11, 12]. In specific, it is believed that the formation and turnover of strong adhesions between the cells and the extracellular matrix (ECM) are indispensable for the generation of intracellular forces to drive cell motility. Interestingly, several recent studies demonstrated that cell-to-ECM adhesion might not be required for cells to move in a confined micro-channel [13, 14]. Instead, it was reported that some cancer cells employ the so-called “osmotic engine” mechanism, the synergistic cooperation of polarly distributed ions and water channel proteins, to propel their forward motion under confinement [14, 15]. In this kind of studies, an osmolarity gradient is often introduced to the cells (by adding or removing salts on one side of the microchannel) to trigger their cell body polarization and migration. However, in such a setting, it is difficult to alter the medium osmolarity rapidly and precisely, and hence to direct the cell migration in a controllable and reversible manner, which could be very useful in future quantitative and mechanistic studies. In addition, it is controversial whether the presence of cell adhesions do facilitate or impede the cell migration under confinement. For example, if cell movement is driven by internal forces generated by the actomyosin-focal adhesion machinery, then stronger adhesion may lead to fast migration of cells. On the other hand, if adhesion is not needed at all for cells to move under confinement, then its presence could actually reduce cell migration. Finally, although it has been reported that the blockade of water channel protein aquaporins diminish tumor cell motility in confined spaces [15], a systematic study on the exact correlation between the aquaporin protein quantity and the migration capability of cells is still lacking.

Here, we report a study aiming at addressing these outstanding issues. Specifically, we developed a novel electro-osmotic hybrid microfluidic system capable of initiating and precisely controlling the cell movements in confined micro-channels. Interestingly, the migration velocity of cells under confinement is strongly influenced by the interactions between the cell body and the channel wall, with stronger adhesions resulting in impaired cell motility. In addition, by examining more than 20 different types of cancer cells, we observed a linear positive correlation between the concentration of aquaporin-4 (AQP4), the most abundant water channel protein in many lung and nasopharyngeal cancer cells [16-18], and cell migration speed. Silencing AQP4 in highly invasive re-populated cancer stem cells reduces cell migration capability down to the level that is comparable to their parental cells. Finally, we demonstrated that such observations can all be quantitatively explained by the "osmotic engine" model where cell-to-microchannel wall adhesion acts as a frictional resistance against cell movement.

2. An electro-osmotic microfluidic system for single cell migration control

The design of our electro-osmotic microfluidic system is shown in Fig. 1A. Basically, the medium bath connected to one side of micro-channels (see Supplementary Materials A for details of channel fabrication) was divided into two compartments by a Nafion membrane film. Given that only cations are allowed to pass through the Nafion membrane, a DC supply can then be used to create a potential difference between two compartments and consequently change the medium osmolarity (see Supplementary Materials A for the calibrated relationship between the applied voltage and major ion concentrations in the medium). Such imposed osmolarity gradient will then trigger the directional movement of cells confined in micro-channels (refer to the inset of Fig. 1A). A representative migration trajectory of A549 cells under the applied voltage, 5V for 1 hour and then switched to -5V for another hour, is shown in Fig. 1B. Interestingly, it was found that cells reversed their moving direction and more or less returned to their original position after the switching of electric potential. In comparison, no apparent cell movement could be observed when no voltage was applied. The average traveling velocity of cells as a function of the applied voltage is shown in Fig. 1C. Clearly, the cell speed increases with the voltage. Furthermore, it was found that, under an applied voltage of 5V, most of the cells (>90%) move in the same direction inside the microchannel over a period of more than two hours, refer to Supplementary Materials B. Therefore, this voltage was used in the rest of our experimental investigations.

3. Cell-ECM adhesion is associated with the migration under electro-osmotic manipulation

As mentioned earlier, although cell-ECM attachment and associated actomyosin contraction have been found to be not indispensable for cells to migrate in confined micro-channels [13-15], whether cell motility will be enhanced or suppressed by the presence of adhesion remains unclear. To answer this important question, we coated the channel wall with pure BSA as well as strong adhesive ligands -fibronectin and collagen I (Supplementary Materials – B) and then compared the corresponding moving capability of A549 cells (a human alveolar adenocarcinoma cell line that is widely used in the study of lung cancer [19]), refer to Fig. 2A. Interestingly, it was found that, in comparison to fibronectin or collagen I coating, cells moved much faster in BSA coated channels. To understand this, the adhesion strength between cells and different coated surfaces were characterized via optical pulling test [20]. Specifically, polystyrene beads coated with these adhesion proteins (under the same coating protocol and protein concentrations) were moved into contact with live A549 cells, allowing adhesion to form, and then pulled away by an optical trap (see Fig. 2B and Supplementary Materials – C and D for details). The measured adhesion energies for all three cases are shown in Fig. 2C. As expected, stronger adhesions were formed between the cell and surfaces coated with fibronectin and Collagen I. As this point, it is clear that the migration capability of cells in confined micro-channels will be reduced by cell-ECM adhesion.

4. Knockdown of AQP4 reduces cancer cell migration under electro-osmotic manipulation

According to the osmotic engine picture [15], cells use polarly distributed ion and water pump/channel proteins to actively transport ion and water molecules across their membrane and propel themselves inside the micro-channel. Therefore, it is reasonable to believe that the migration capability of cells is AQP-dependent. Following this line of reasoning, the migration speed of five types of nasopharyngeal and lung cancer cells (refer to Supplementary Materials – E), with distinct AQP-4 concentrations, were measured in our experimental setup. Note that, here we focused on AQP-4 because it has been shown recently that it is the most abundant species among different aquaporins in nasopharyngeal and lung cancer cells [18]. Interestingly, as shown in Fig. 3A and 3B, cells with more AQP-4 were migrating faster. In addition, knockdown of AQP4 in A549 cells via siRNA (Supplementary Materials – F) reduced their sped to the level comparable to their normal counterpart (i.e. NP69 cells).

5. Cell migration speed increased with cancer-stemness under electro-osmotic

manipulation

Another interesting issue that can be examined by our system is the invasiveness characterization of the so-called cancer stem cells, which are believed to act as initiating targets for development of cancers [21-23] and potentially drive cancer progression [22, 24]. Here, following well-established protocols [22, 23], cancer stem cells were developed from different (H23, A549 and H3255) parental lung cancer cell lines, as confirmed by an increased expression of Sox-2 and Oct-4 (both as stem cell-like markers) in Western blotting (Fig. 4A-C, and see Supplementary Materials H for densitometric quantification). In particular, the concentration was normalized by that of the loading control marker GAPDH to determine the relative differences between different proteins. The moving trajectories of these cancer stem cells in the micro-channel are shown in Fig. 4A-C. Interestingly, once the concentration of AQP4 was suppressed via siRNA, the migration capabilities of these cancer stem cells were greatly reduced to those that are comparable to their corresponding parent cells (Fig. 4A-C). In addition, under such circumstance, the concentration of Sox-2 or Oct-4 was also significantly reduced.

The correlation between AQP4 concentration and the average traveling velocity is best summarized in Fig. 5 where more than 20 types of cells were tested in collagen I coated micro-channels. Clearly, our data suggest that the migration capability of cells in a confined environment approximately increases linearly with respect to their AQP4 concentration (relative to the loading control GAPDH).

6. Effect of cell migration speed with AQP levels across cell types

The recently developed osmotic engine model [15] was adopted here to explain our experimental observations (see Supplementary Materials I for detailed description of the model). According to this theory, the steady speed (V) of cells trapped in a micro-channel can be estimated as

$$V = \frac{b^2 h\alpha\{2D(\Pi_{out,b} - \Pi_{out,f}) + LRT[\gamma(\Delta\Pi_{c,f} - \Delta\Pi_{c,b}) + \beta(\sigma_{c,f} - \sigma_{c,b})]\}}{6bL^2RT\alpha\beta\eta + 12hL\alpha\eta(2D + LRT\gamma) + b^2[4Dh + LRT(2h\gamma + L\alpha\beta\zeta_w)]} \quad (1)$$

where b is the width of microchannel, L represents the cell length, h corresponds to the thickness of the cell cortical layer, η stands for the cytoplasm viscosity, R is the molar gas constant and T is absolute temperature. Within this picture, cell movement is driven by the polarly distributed AQPs and ion transporters, leading to a biased cross-membrane ion/water flux at the leading and trailing edge of cells. To take into account

these features, a set of parameters - D, α, β and γ are introduced in Eq. (1) which correspond to the diffusivity of ions, exchange rate of water molecules and the rate constant of ion flux through mechanosensitive channels and ion transporters, respectively [15]. In addition, Π_{out} and $\Delta\Pi_c$ represent the medium osmolarity and the threshold osmotic pressure of the cell while the subscript "f" and "b" refer to the front (leading) and back (trailing) edge of the cell. Finally, possible resistance by the channel on cell movement is characterized by the friction coefficient ζ_w.

To make a connection to our actual tests, the values of ζ_w, α and L were varied according to different experimental conditions. Specifically, ζ_w was assumed to be proportional to the measured adhesion strength between the cell and the coated channel surface (Fig. 2C). Furthermore, since the AQP concentration and cell length could be different in each cell line and under different treatment conditions, the values of α and L were also varied according to the measured AQP concentration and cell size in each case respectively (see Supplementary Materials – I for more details). Notice that, as a reference, ζ_w and α for A549 cells under BSA coating were taken to be 6.5×10^8 Pa. s/m and 0.36×10^{-12} m Pa^{-1} s^{-1}, respectively, which are comparable to those ($\zeta_w = 8 \times 10^8$ Pa. s/m and $\alpha = 1 \times 10^{-12}$ m Pa^{-1} s^{-1}) adopted in [15] for sarcoma cancer S180 cells confined in micro-channels without coating of adhesion proteins.

Interestingly, choosing realistic parameters as shown in Table S1-4 in the Supplementary Materials I, the predicted trajectories of cells match well with our experimental observations under different cell-channel adhesion strength (Fig. 2A). In addition, the traveling velocities of different cells calculated from their measured length and AQP4 concentration (i.e. different L and α values as shown in Table S2 and Table S3), are also in agreement with our experiments (Fig. 5). Specifically, the shaded region in Fig. 5 represents the range of the predicted cell speed when the cell length is allowed to vary by ±30% from the measured mean value (Table S2). Note that, since all results shown in Fig. 5 were based on collagen I coated channels ζ_w was fixed as 36×10^8 Pa.s/m (Table S4) in this case.

7. Summary and future work

In this study, an electro-osmotic microfluidic device was developed to characterize the moving capability of tumor cells in a confined environment. Compared to other systems developed before, the moving speed and direction of the cell can all be easily controlled by an applied voltage in our setup. Using this device, it was found that the moving velocity of cells is strongly influenced by the interactions between the cell and the

channel wall, with a stronger adhesion resulting in diminished cell motility. It must be pointed out that although previous studies have demonstrated that adhesion is not required for the cell to move in micro-channels, how interactions between cells and channel wall affect their migration capability remains unclear [12-14, 25]. Here, we unambiguously showed that cell-channel adhesion works as a resisting factor against the movement of cells. In addition, given the versatility of our system, it is conceivable that this setup can serve as a powerful tool in investigating how other factors, like the rigidity of channel wall [26-28], galvanotaxis [29], pressure [30, 31] and the surrounding electrical field [29, 32] influence the movement and related process (such as growth and proliferation) of cells, as well as the mechanisms behind, in the future.

By examining more than 20 different types of tumor cells, we also showed that the moving speed of cells increases almost linearly with their concentration of aquaporin-4 (AQP4). In particular, knockdown of AQP4 in highly invasive re-populated cancer stem cells reduced their migration capability to the level that is comparable to their parental cell lines, indicating the potential such channel protein as a therapeutic target [16, 33]. Indeed, few pharmacological modulators of AQPs are available now, however they are either composed of heavy metals that are known to lack specificity or are toxic [33, 34]. In this regard, we believe that the robust system developed here could also be useful in facilitating the of process of identifying suitable AQP (or other target proteins) inhibitors that aim at limiting the motility/invasiveness of tumor cells and eventually treating cancer. Another possible application could be the sorting of cancer stem cells, i.e. to select cancer cells with greater stemness out of a heterogeneous mixture of tumor cells.

Finally, it must be pointed out that the real situation of cell migration in vivo could be much more complicated than what have been considered in this study. For example, a cancer cell may interact with neighboring cells during its movement while the surrounding tissue usually has a micro-porous architecture. How to incorporate these important features in the present experimental setup is certainly something that warrants further investigation. In addition, the migration capabilities of different cell lines were examined separately here. It will be interesting to see whether similar conclusions can also be obtained if multiple cell types are tested simultaneously (i.e. under exactly the same environmental parameters) in the electro-osmolarity migration assay developed. Studies along these lines are currently underway.

Acknowledgement

This work was supported by grants from the Research Grants Council (Project Nos. HKU 17205114, HKU 17211215, HKU 17257016) of the Hong Kong Special Administration Region and the National Natural Science Foundation of China (Project No. 11572273, 11622222 and 11472271). H.J. also acknowledges the support from the Strategic Priority Research Program of the Chinese Academy of Sciences (Grant No. XDB22040403).

Author contributions

Y.L., H.J. and Z.G. conceived the study. T.H.H., H.W.F., M.Y. and K.W.K. performed experiments. T.H.H., W.C.C., K.C.N., K.H.W., Y.T., S.Y. and Y.L. analyzed data. T.H.H. Y.L., H.J. and Z.G. wrote the manuscript. All authors reviewed the manuscript.

References

[1] Jimenez, L., Jayakar, S.K., Ow, T.J. & Segall, J.E. 2015 Mechanisms of Invasion in Head and Neck Cancer. Archives of pathology & laboratory medicine 139, 1334-1348. (doi:10.5858/arpa.2014-0498-RA).

[2] Gritsenko, P.G., Ilina, O. & Friedl, P. 2012 Interstitial guidance of cancer invasion. The Journal of pathology 226, 185-199. (doi:10.1002/path.3031).

[3] Lugassy, C. & Barnhill, R.L. 2007 Angiotropic melanoma and extravascular migratory metastasis: a review. Advances in anatomic pathology 14, 195-201. (doi:10.1097/PAP.0b013e31805048d9).

[4] Justus, C.R., Leffler, N., Ruiz-Echevarria, M. & Yang, L.V. 2014 In vitro Cell Migration and Invasion Assays. Journal of Visualized Experiments : JoVE, 51046. (doi:10.3791/51046).

[5] Boussommier-Calleja, A., Li, R., Chen, M.B., Wong, S.C. & Kamm, R.D. 2016 Microfluidics: A new tool for modeling cancer-immune interactions. Trends in cancer 2, 6-19. (doi:10.1016/j.trecan.2015.12.003).

[6] Lanz, H.L., Saleh, A., Kramer, B., Cairns, J., Ng, C.P., Yu, J., Trietsch, S.J., Hankemeier, T., Joore, J., Vulto, P., et al. 2017 Therapy response testing of breast cancer in a 3D high-throughput perfused microfluidic platform. BMC Cancer 17, 709. (doi:10.1186/s12885-017-3709-3).

[7] Paguirigan, A.L. & Beebe, D.J. 2008 Microfluidics meet cell biology: bridging the gap by validation and application of microscale techniques for cell

biological assays. BioEssays : news and reviews in molecular, cellular and developmental biology 30, 811. (doi:10.1002/bies.20804).

[8] Sackmann, E.K., Fulton, A.L. & Beebe, D.J. 2014 The present and future role of microfluidics in biomedical research. Nature 507, 181. (doi:10.1038/nature13118).

[9] Chen, Z. & Zhao R., 2019 Engineered Tissue Development in Biofabricated 3D Geometrical Confinement–A Review. ACS Biomater. Sci. Eng., Article ASAP. (10.1021/acsbiomaterials.8b01195)

[10] Kuzmic, N., Moore. T., Devadas, D & Young, E.W.K. 2019 Modelling of endothelial cell migration and angiogenesis in microfluidic cell culture systems. Biomech Model Mechanobiol. (10.1007/s10237-018-01111-3)

[11] Paul, C.D., Mistriotis, P. & Konstantopoulos, K. 2017 Cancer cell motility: lessons from migration in confined spaces. Nature reviews. Cancer 17, 131-140. (doi:10.1038/nrc.2016.123).

[12] Lee, S. & Kumar, S. 2016 Actomyosin stress fiber mechanosensing in 2D and 3D. F1000Research 5, F1000 Faculty Rev-2261. (doi:10.12688/f1000research.8800.1).

[13] Balzer, E.M., Tong, Z., Paul, C.D., Hung, W.C., Stroka, K.M., Boggs, A.E., Martin, S.S. & Konstantopoulos, K. 2012 Physical confinement alters tumor cell adhesion and migration phenotypes. Faseb j 26, 4045-4056. (doi:10.1096/fj.12-211441).

[14] Stroka, K.M., Gu, Z., Sun, S.X. & Konstantopoulos, K. 2014 Bioengineering paradigms for cell migration in confined microenvironments. Curr Opin Cell Biol 30, 41-50. (doi:10.1016/j.ceb.2014.06.001).

[15] Stroka, Kimberly M., Jiang, H., Chen, S.-H., Tong, Z., Wirtz, D., Sun, Sean X. & Konstantopoulos, K. 2014 Water Permeation Drives Tumor Cell Migration in Confined Microenvironments. Cell 157, 611-623. (doi:10.1016/j.cell.2014.02.052).

[16] Verkman, A.S., Anderson, M.O. & Papadopoulos, M.C. 2014 Aquaporins: important but elusive drug targets. Nat Rev Drug Discov 13, 259-277. (doi:10.1038/nrd4226).

[17] Warth, A., Muley, T., Meister, M., Herpel, E., Pathil, A., Hoffmann, H., Schnabel, P., Bender, C., Buness, A., Schirmacher, P., et al. 2011 Loss of aquaporin-4 expression and putative function in non-small cell lung cancer. BMC Cancer 11, 161. (doi: 10.1186/1471-2407-11-161)

[18] Hui, T.H., Kwan, K.W., Yip, T.T.C., Fong, H.W., Ngan, K.C., Yu, M., Yao, S., Ngan, A.H.W. & Lin, Y. 2016 Regulating the Membrane Transport Activity and Death of Cells via Electroosmotic Manipulation. Biophys J 110, 2769-2778. (doi:10.1016/j.bpj.2016.05.011).

[19] Lieber M, Smith B, Szakal A, Nelson-Rees W, Todaro G. A continuous tumor-cell line from a human lung carcinoma with properties of type II alveolar

epithelial cells. International journal of cancer Journal international du cancer 1976;17(1):62-70.

[20] Hui, T.H., Zhu, Q., Zhou, Z.L., Qian, J. & Lin, Y. 2014 Probing the coupled adhesion and deformation characteristics of suspension cells. Applied Physics Letters 105. (doi:doi:http://dx.doi.org/10.1063/1.4893734).

[21] Kim, C.F., Jackson, E.L., Woolfenden, A.E., Lawrence, S., Babar, I., Vogel, S., Crowley, D., Bronson, R.T. & Jacks, T. 2005 Identification of bronchioalveolar stem cells in normal lung and lung cancer. Cell 121, 823-835. (doi:10.1016/j.cell.2005.03.032).

[22] Tan, Y., Tajik, A., Chen, J., Jia, Q., Chowdhury, F., Wang, L., Chen, J., Zhang, S., Hong, Y., Yi, H., et al. 2014 Matrix softness regulates plasticity of tumour-repopulating cells via H3K9 demethylation and Sox2 expression. Nat Commun 5. (doi:10.1038/ncomms5619).

[23] Liu, J., Tan, Y., Zhang, H., Zhang, Y., Xu, P., Chen, J., Poh, Y.C., Tang, K., Wang, N. & Huang, B. 2012 Soft fibrin gels promote selection and growth of tumorigenic cells. Nature Materials 11, 734. (doi:10.1038/nmat3361).

[24] Visvader, J.E. & Lindeman, G.J. 2012 Cancer Stem Cells: Current Status and Evolving Complexities. Cell Stem Cell 10, 717-728. (doi:https://doi.org/10.1016/j.stem.2012.05.007).

[25] Li, Y. & Sun, S.X. 2018 Transition from Actin-Driven to Water-Driven Cell Migration Depends on External Hydraulic Resistance 114(12):2965-2973 (doi: 10.1016/j.bpj.2018.04.045)

[26] Shenoy, V.B., Wang, H. & Wang, X. 2016 A chemo-mechanical free-energy-based approach to model durotaxis and extracellular stiffness-dependent contraction and polarization of cells. Interface focus 6, 20150067. (doi:10.1098/rsfs.2015.0067).

[27] Gao, H., Qian, J. & Chen, B. 2011 Probing mechanical principles of focal contacts in cell-matrix adhesion with a coupled stochastic-elastic modelling framework. Journal of the Royal Society, Interface 8, 1217-1232. (doi:10.1098/rsif.2011.0157).

[28] Hui, T.H., Tang, Y.H., Yan, Z., Yip, T.T.C., Fong, H.W., Cho, W.C., Ngan, K.C., Shum, H.C. & Lin, Y. 2018. Cadherin- and Rigidity-Dependent Growth of Lung Cancer Cells in a Partially Confined Microenvironment. ACS Biomaterials Science & Engineering. 4: 446-455.

[29] Mycielska, M.E. & Djamgoz, M.B. 2004 Cellular mechanisms of direct-current electric field effects: galvanotaxis and metastatic disease. J Cell Sci., 1, 117(Pt 9): 1631-9 (doi: 10.1242/jcs.01125)

[30] Taloni, A., Amar, B.M., Zapperi, S. & La Porta, C.A.M. 2015 The role of pressure in cancer growth, Eur. Phys. J. Plus 130(224). (doi.org/10.1140/epjp/i2015-15224-0)

[31] Hui, T.H., Zhou, Z.L., Qian, J., Lin, Y., Ngan, A.H.W. & Gao, H. 2014. Volumetric Deformation of Live Cells Induced by Pressure-Activated Cross-Membrane Ion Transport. Physical Review Letters. 113: 118101.

[32] Witek, M.A., Wei, S., Vaidya, B., Adams, A.A., Zhu, L., Stryjewski, W., McCarley, R.L. & Soper, S.A. 2004 Cell transport via electromigration in polymer-based microfluidic devices. Lab on a Chip 4, 464-472. (doi:10.1039/B317093D).

[33] Wang, J., Feng, L., Zhu, Z., Zheng, M., Wang, D., Chen, Z. & Sun, H. 2015 Aquaporins as diagnostic and therapeutic targets in cancer: How far we are? Journal of Translational Medicine 13, 96. (doi:10.1186/s12967-015-0439-7).

[34] Tradtrantip, L., Jin, B.J., Yao, X., Anderson, M.O. & Verkman, A.S. 2017 Aquaporin-Targeted Therapeutics: State-of-the-Field. Advances in experimental medicine and biology 969, 239-250. (doi:10.1007/978-94-024-1057-0_16).

List of Figures

Figure 1: (A) – Schematics of the electro-osmotic system. The medium bath connected to one side of micro-channels is divided into two compartments by a Nafion membrane film. A DC supply is used to create a potential difference between two compartments and consequently introduce a osmolarity gradient to cells in the micro-channels as well as trigger their movement. The movement of an A549 cell inside a 7-μm microchannel is shown in the inset where images were taken at every 10 minutes. Here a voltage of +5V was applied for 60 minutes before switching to -5V for another 60 minutes. (B) – Average moving trajectory of A549 cells under the voltage signal described in (A). Data shown here are based on 10 independent tests with $p<0.05$ (from student t-test) and error bar represents the standard deviation of the measurements. (C) The measured average traveling cell velocity, calculated from the slope of the moving trajectory of cells, as a function of the amplitude of the applied voltage.

Figure 2: (A) – Images showing the movement of A549 cells in the 7-μm microchannel coated with Bovine Serum Albumin (BSA), Fibronectin and Collagen I under an applied voltage of +5V (Left). The corresponding moving trajectories (averaging from 10 independent tests) are given on the right, where predictions from Eq. (1) are shown by the solid line. (B) Schematic diagram of using an optical-tweezers setup to quantify the adhesion strength between a cell and a coated surface (Left). Time-lapsed images on the right showing a coated bead, initially adhering to a A549 cell, was pulled away from the cell by the Optical Tweezers. (C) – Beeswarm plot illustrating the measured relative adhesion energy density between A549 cells and the BSA, Fibronectin or Collagen I coated surface. Data shown here are based on 5 independent experiments where a statistical significance of $p < 0.05$ (from student t-test between different coating groups) has been achieved and error bar represents the standard deviation of the measurements.

Figure 3: (A) Movement of C666, A549, HK1, A549 with AQP4 silenced and NP69 cells in the confined microchannel under an applied voltage of +5V. Error bars represent the standard deviations of the measurements (B) Beeswarm plots showing the average traveling velocity of cells along with their corresponding AQP concentrations. The AQP concentration was quantified (from 5 independent Western blots) by comparing its value to that of the loading control marker, GAPDH.

Figure 4: Western blots (Left) and moving trajectories (Right) of (A) H23, (B) A549 and (C) H3255 cells. Here, results from each type of cells, their isolated stem cells and

corresponding cells with AQP4 knocked out are shown together. The protein concentration of AQP4, the stem-cell markers Sox-2 and Oct-4, and the control marker GAPDH were all measured from 10 independent Western blots (refer to Supplementary Materials H for details of quantitative measurement). Error bar represents the standard deviation of the measurements.

Figure 5: Relationship between the measured AQP4 concentration and the average traveling velocity of cells in collagen I coated micro-channel. The AQP4 concentration is normalized by that of the loading control marker, GAPDH. 8 independent measurements (on both the AQP4 concentration and cell speed) were conducted for each phenotype and error bar indicates the standard deviation of the measurements. The shaded region represents the range of the predicted cell speed from Eq. (1) when the cell length is allowed to vary by ±30% from the measured mean value (Table S2). Here, the values of α for different cell types were chosen according to Table S3 while ζ_w was fixed as 36×10^8 Pa.s/m (corresponding to collagen I coating, refer to Table S4).

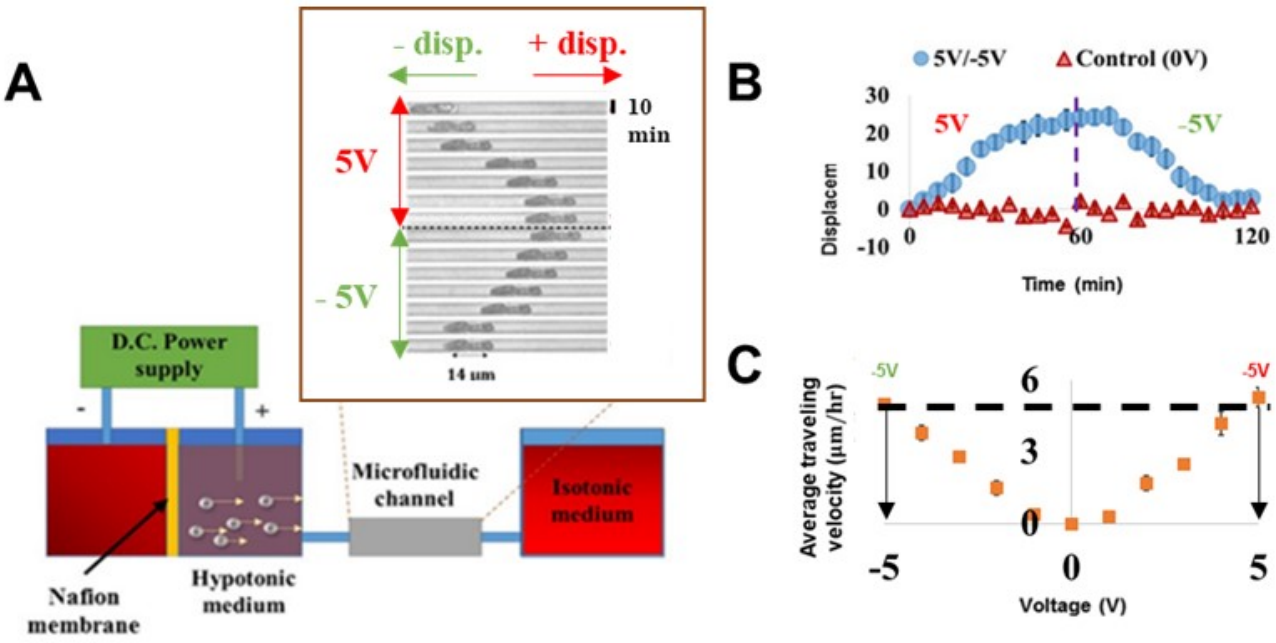

Figure 1

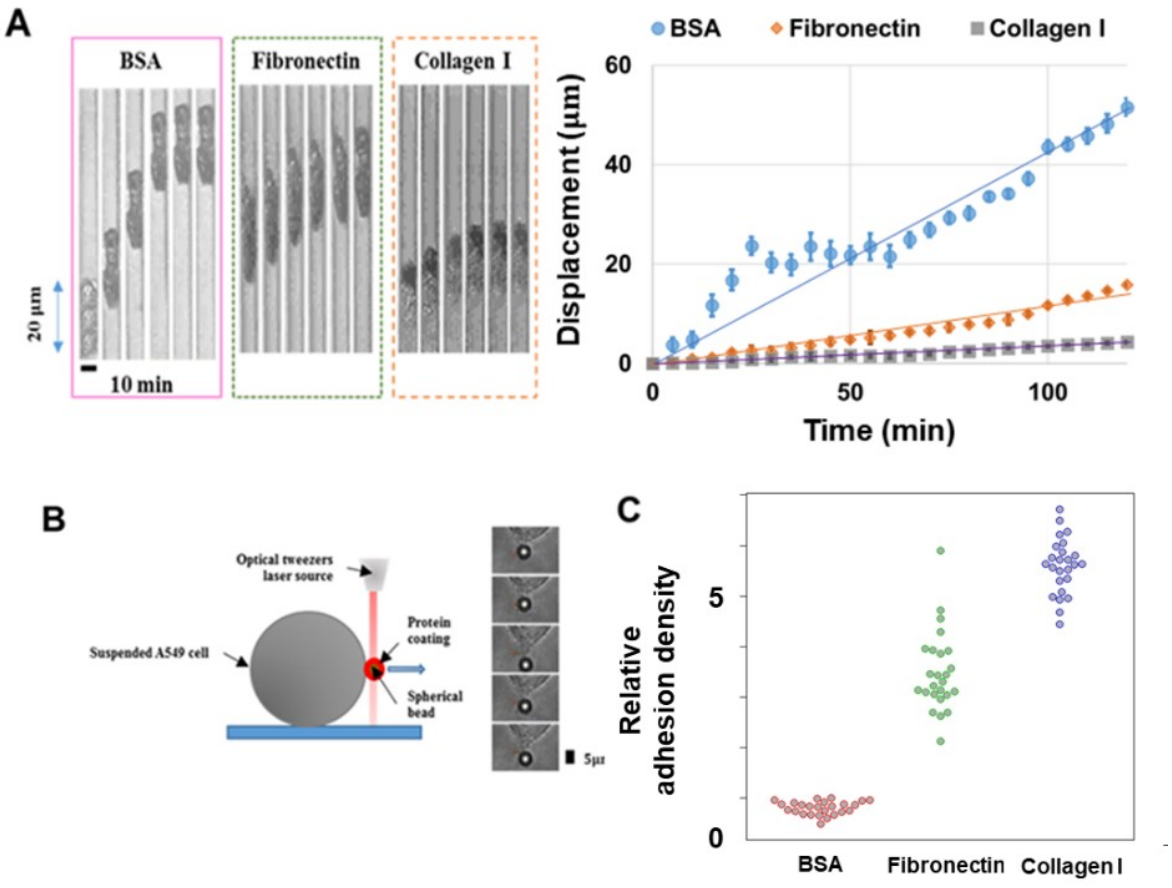

Figure 2

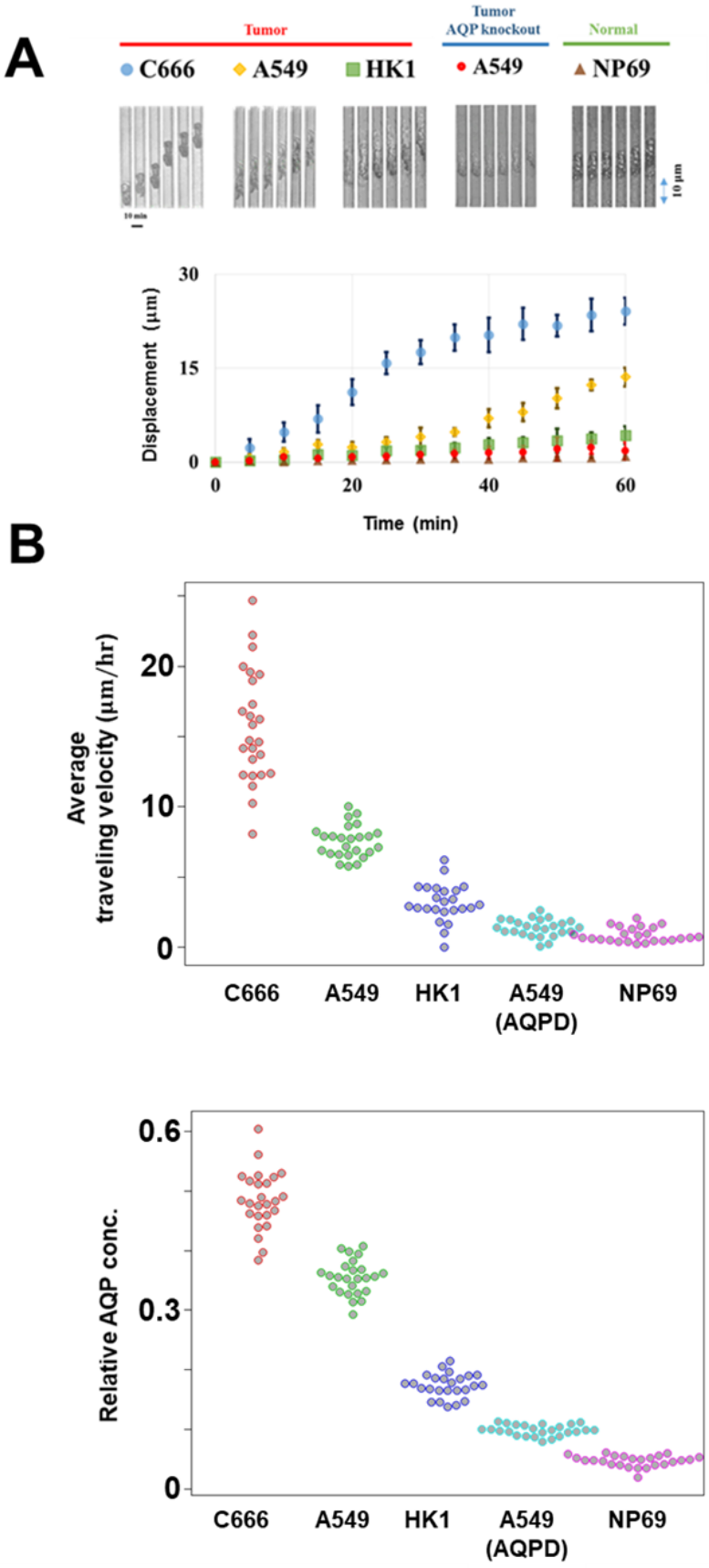
A
Tumor
Tumor
AQP knockout
Normal
C666
A549
HK1
A549
NP69
10 μm
Displacement (μm)
30
15
0
0
20
40
60
Time (min)
B
Average
traveling velocity (μm/hr)
20
10
0
C666
A549
HK1
A549
(AQPD)
NP69
Relative AQP conc.
0.6
0.3
0
C666
A549
HK1
A549
(AQPD)
NP69

Figure 3

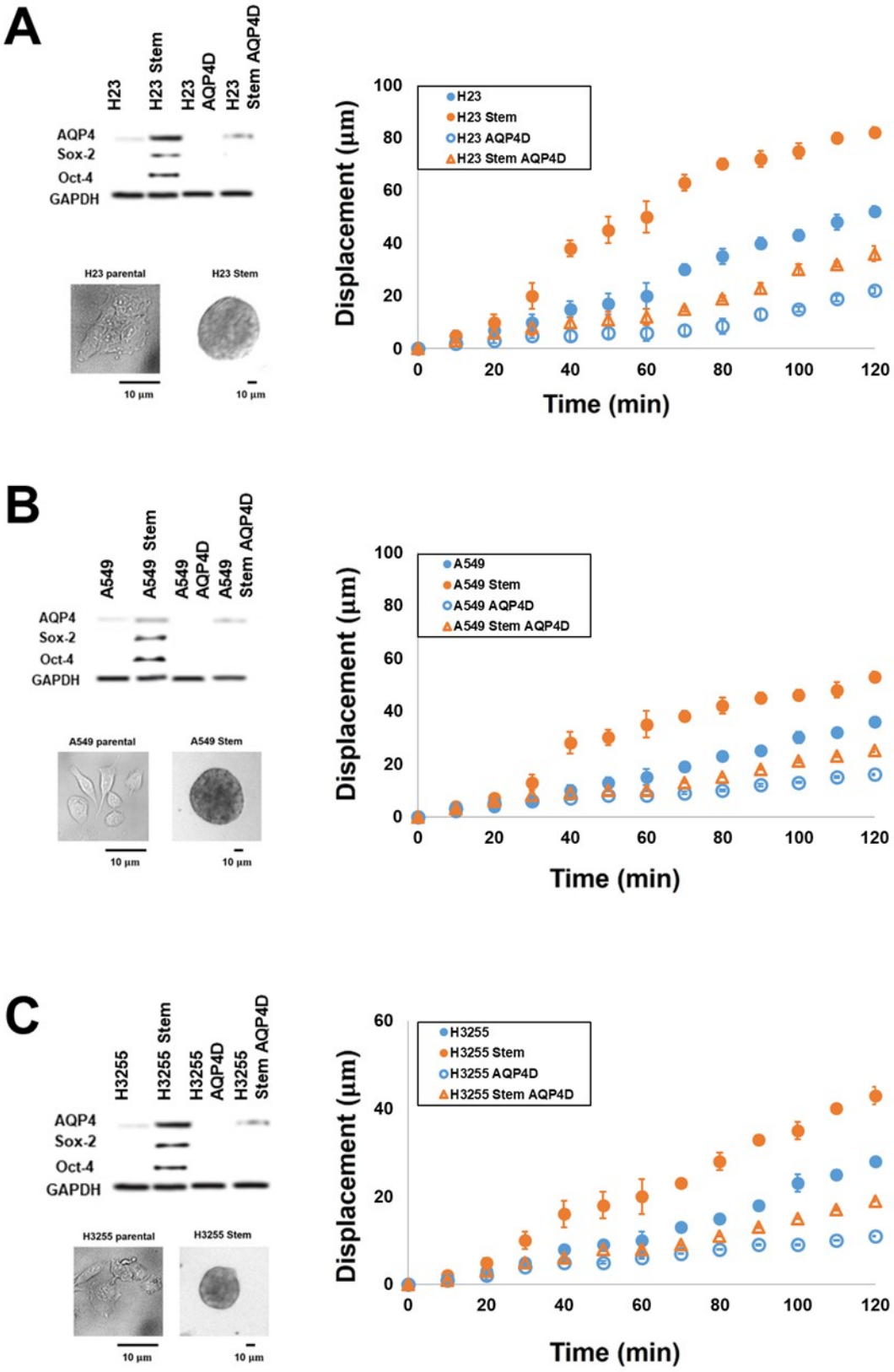
A
H23
H23 Stem
H23 AQP4D
H23 Stem AQP4D
AQP4
Sox-2
Oct-4
GAPDH
H23 parental
H23 Stem
10 μm
10 μm
Displacement (μm)
H23
H23 Stem
H23 AQP4D
H23 Stem AQP4D
Time (min)
B
A549
A549 Stem
A549 AQP4D
A549 Stem AQP4D
AQP4
Sox-2
Oct-4
GAPDH
A549 parental
A549 Stem
10 μm
10 μm
Displacement (μm)
A549
A549 Stem
A549 AQP4D
A549 Stem AQP4D
Time (min)
C
H3255
H3255 Stem
H3255 AQP4D
H3255 Stem AQP4D
AQP4
Sox-2
Oct-4
GAPDH
H3255 parental
H3255 Stem
10 μm
10 μm
Displacement (μm)
H3255
H3255 Stem
H3255 AQP4D
H3255 Stem AQP4D
Time (min)

Figure 4

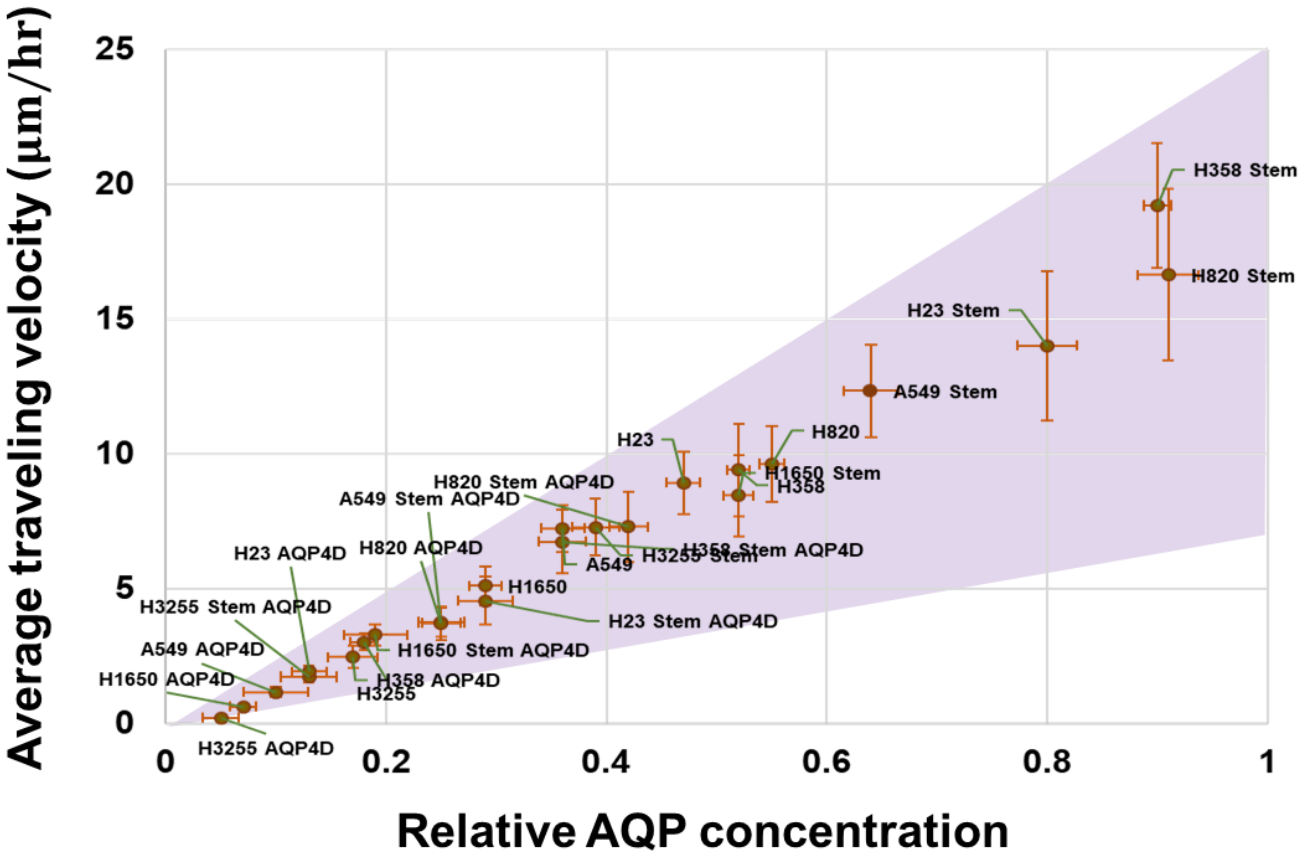
Average traveling velocity (μm/hr)
25
20
15
10
5
0
0
0.2
0.4
0.6
0.8
1
Relative AQP concentration
H358 Stem
H820 Stem
H23 Stem
A549 Stem
H820
H23
H1650 Stem
H358
H820 Stem AQP4D
A549 Stem AQP4D
H23 AQP4D
H820 AQP4D
A549
H3255 Stem
H359 Stem AQP4D
H1650
H23 Stem AQP4D
H3255 Stem AQP4D
A549 AQP4D
H1650 Stem AQP4D
H1650 AQP4D
H358 AQP4D
H3255
H3255 AQP4D

Figure 5